Perseus in Sicily: From Black Hole to Cluster Outskirts
Proceedings IAU Symposium No. 342, 2018
K. Asada, E. de Gouveia Dal Pino, M. Giroletti,
H. Nagai & R. Nemmen, eds.

doi:10.1017/S1743921318005756

Deep Chandra observations of the core of the Perseus cluster

Jeremy S. Sanders

Max-Planck-Institut für extraterrestrische Physik,
Giessenbachstr. 1, 85748 Garching, Germany
email: jsanders@mpe.mpg.de

Abstract. The Perseus cluster is the X-ray brightest cluster in the sky and with deep Chandra observations we are able to map its central structure on very short spatial scales. In addition, the high quality of X-ray data allows detailed spatially-resolved spectroscopy. In this paper I review what these deep observations have told us about AGN feedback in clusters, sloshing and instabilities, and the metallicity distribution.

Keywords. galaxies: clusters: individual (Perseus cluster, Abell 426)

1. Introduction

The Perseus cluster is the X-ray-brightest galaxy cluster in the sky. The central galaxy, NGC 1275 contains the well-known radio source 3C 84. It is also the prototypical 'cool core' cluster, showing short central cooling times. Given its proximity ($z \sim 0.018$) and brightness, the cluster is an ideal location to study the interaction of an active galactic nucleus (AGN) with its surroundings.

The Chandra X-ray observatory (Weisskopf *et al.* 2002) was launched in 1999. With its sub-arcsecond spatial resolution it has revealed an increasing amount of detail in a series of increasingly deep observations of Perseus. The initial findings in 24 ks of data were reported in Fabian *et al.* (2000), with deeper observations totalling ~ 200 ks in Fabian *et al.* (2003a), and very deep observations totalling ~ 900 ks in Fabian *et al.* (2006). This was later followed by 500 ks of wider-field observations making use of the Chandra ACIS-I array (Fabian *et al.* 2011).

2. The central cavities and shock

Galaxy clusters are filled with a hot X-ray emitting plasma, the intracluster medium (ICM), which dominates the baryonic component. Using ROSAT, Böhringer *et al.* (1993) observed that there were two central cavities in the X-ray emission. These cavities were coincident with the radio lobes or bubbles of the central radio source 3C 84. As the jets from the nucleus impact with the ICM, the bubbles are formed. The thermal ICM is displaced by the material in the bubbles, leading to cavities in the X-ray emission. Fabian *et al.* (2000) revealed these cavities with Chandra observations in much greater detail. Since then, they have been discovered in the majority of nearby clusters with short central cooling times (for a review see Fabian 2012). This is important because in many of these systems the ICM would be rapidly cooling in the centre, but evidence for this is not seen in their X-ray spectra or at other wavelengths. Energetically, the enthalpy of the material in the bubbles ($4PV$ if relativistic; Churazov *et al.* 2002) could be available to replace the energy lost by cooling. Indeed, if the heating power (calculated

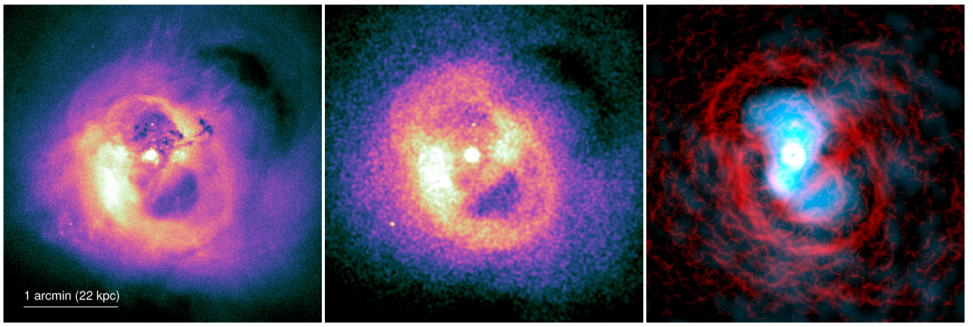

Figure 1. (Left panel) Full band image of the centre of Perseus. (Middle panel) Pressure sensitive, 3.5 to 8 keV image. (Right panel) Edge-filtered 3.5 to 8 keV image in red, with 330 MHz radio overlayed in cyan. North is to the top and east is to the left in images unless otherwise noted.

from the enthalpy and assuming some timescale) is compared to the cooling luminosity for a sample of clusters and groups, there is good agreement.

Fig. 1 (left panel) shows the Chandra image of the centre of the cluster. Either side of the nucleus are the cavities in the X-ray emission. In this image are also soft filaments (discussed in Section 4) and the shadow of a galaxy along the line of sight to the galaxy cluster blocking out soft X-rays (Gillmon *et al.* 2004; Sanders & Fabian 2007). The cavities can be seen more clearly in a hard X-ray image which is more sensitive to X-ray thermal pressure rather than density variations (Fig. 1 centre panel). We have applied an edge filtering technique (Gaussian Gradient Magnitude or GGM) to filter X-ray images to be sensitive to gradients in the X-ray surface brightness (Sanders *et al.* 2016). The pressure-sensitive edge-filtered image is shown in Fig. 1 (right panel), overplotting an image of the 330 MHz radio emission from the radio bubbles.

Fabian *et al.* (2000) found that the material in the bright X-ray emitting rims of the cavities was around 3 keV in projected temperature, cooler than the surrounding 4 keV ICM. Beyond the bright cavity rims, Fabian *et al.* (2003a) identified the thick shell around the northern cavity as a weak shock with a Mach number of around 1.5. There is also likely a second shock around the southern cavity, although the projected cooler material makes this harder see (Fig. 1 centre and right panels show the second southern shock more clearly). The inflation of the central cavities by the radio jet is therefore shocking the surrounding ICM. Although there is a clear density and pressure jump, surprisingly there was not the expected temperature jump across the edge (Graham *et al.* 2008). Possible explanations for the lack of temperature jump include mixing of cooler filamentary gas at the shock (the filaments abruptly end at the shock front). If the material in the bubbles is relativistic, it can release its $4PV$ enthalpy into the ICM, where V is the cavity volume (estimated from the area on the sky) and P is the pressure of the material (inferred from the pressure of the surrounding X-ray emitting gas assuming it is close to pressure equilibrium). Graham *et al.* (2008) measured $3.5PV$ excess energy in the shocked region, close to the cavity enthalpy.

To the north-west of the image is visible a third cavity, previously seen in Einstein observatory images (Fabian *et al.* 1981; Branduardi-Raymont *et al.* 1981). There is another cavity outside the image to the south. These outer cavities are seen in low frequency emission (Fabian *et al.* 2002). These bubbles were likely formed in an earlier outburst of the central nucleus and have buoyantly risen in the gravitational potential of the cluster.

https://doi.org/10.1017/S1743921318005756 Published online by Cambridge University Press

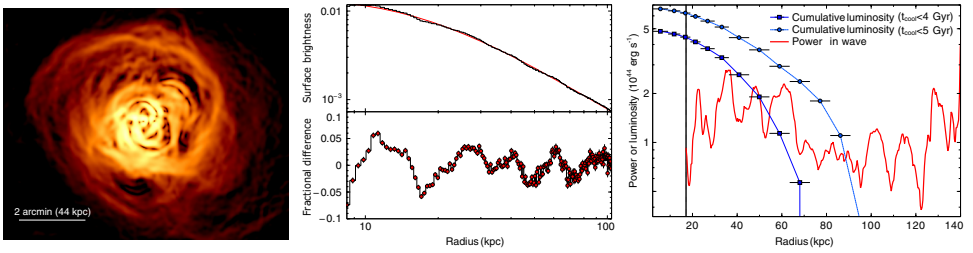

Figure 2. (Left panel) GGM-filtered X-ray image of Perseus, showing gradients on 4 arcsec (1.5 kpc) scales. (Centre panel) Surface brightness profile along an east-southeast sector (Sanders & Fabian 2007) and residuals to a smooth model. (Right panel) Sound wave power as a function of radius, if they are generating the observed surface brightness fluctuations, compared to the cumulative cooling luminosity in regions where the cooling time is < 4 or < 5 Gyr, from Sanders & Fabian (2007).

3. Sound waves and feedback

Fabian *et al.* (2003a) discovered a series of surface brightness ripples around the core of the cluster (Fig. 2 left and centre panels). An explanation is that these could be sound waves generated by the central AGN feedback. If this is the case, then if they can be dissipated in the ICM then they could provide a mechanism by which the AGN could heat the core of the cluster in a distributed fashion. Sound waves are seen in simulations of AGN feedback (e.g. Ruszkowski *et al.* 2004; Sijacki & Springel 2006).

Sanders & Fabian (2007) calculated the energy in the ripples assuming that they are spherical sound waves (Fig. 2 right panel). The sound waves can carry several $10^{44}\,\mathrm{erg\,s^{-1}}$, a substantial fraction of the energy lost by X-ray radiation. Combined with the from weak shocks in the centre, the combination could plausibly heat the cooling region. The amplitude of the ripples has an e-folding decay length of ~ 50 kpc, similar to the radius of the cooling region.

Alternatively, turbulence may be the mechanism by which heating is distributed over the core of the cluster. If the density fluctuations are used to infer turbulence via simulations (Zhuravleva *et al.* 2014), assuming that the fluctuations do not have another origin, there is a good correspondence between the inferred heating rate and the radiative cooling rate in radial bins in Perseus.

If turbulence is responsible it has been noted that the responsible gravity waves travel slowly radially and there is not a great deal of energy in turbulence in Perseus as seen by Hitomi (Fabian *et al.* 2017). The speed of sound is much faster than the gravity wave radial velocity and does not have this problem. Gravity waves would be required to be created at each radius, by cavities for example, to have a close heating-cooling balance. Future deep observations with XRISM and Athena (Croston *et al.* 2013) will tell us in detail what the velocity structure of the gas is in Perseus and other systems, allowing us to know which heating mechanisms are the most important.

4. The filamentary nebula

The core of the cluster contains a well-known filamentary nebula (Kent & Sargent 1979) spanning out to 70 kpc in radius. These filaments are also seen in soft X-rays by Chandra (Fig. 3; Fabian *et al.* 2003b). The morphology of the filaments behind the outer cavity to the north-west suggests that they are tracing the velocity structure of the intracluster medium, as also suggested by their velocity structure (Hatch 2006), although not all the filaments appear to be dragged out by bubbles (Gendron-Marsolais *et al.* 2018). It has been suggested that particle heating may be responsible for the emission of these filaments (Ferland *et al.* 2009).

https://doi.org/10.1017/S1743921318005756 Published online by Cambridge University Press

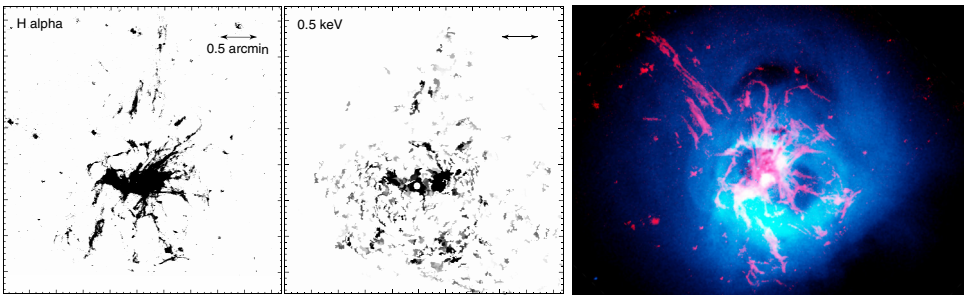

Figure 3. (Left and centre panels) Comparison of the Hα nebula with the X-ray emitting gas of a temperature $\sim$0.5 keV (Sanders & Fabian 2007). The X-ray map was made by spectral fitting of gas in regions with a model made up of multiple temperature components. (Right panel) Chandra X-ray image of the cluster in blue with an Hα image of the filaments from Conselice *et al.* (2001) in red, rotated so that the outer bubble is upwards.

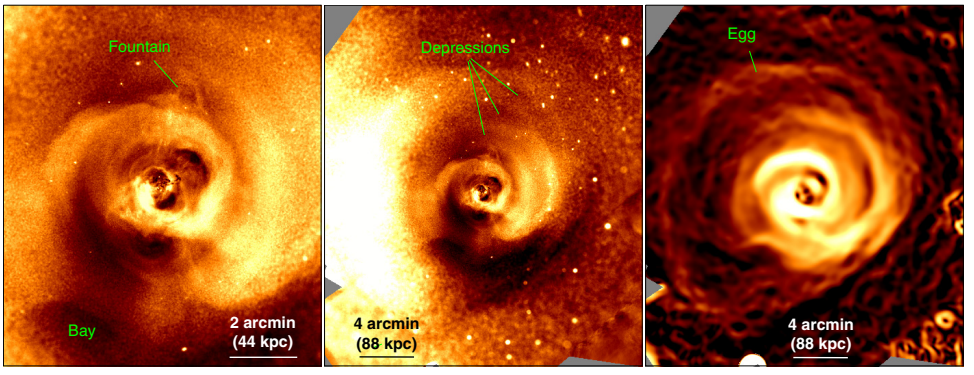

Figure 4. (Left panel) Adaptively-smoothed image of the cluster, showing the fractional difference from the average surface brightness at each radius. (Centre panel) Zoomed-out image of the fractional difference from each radius. (Right panel) GGM-filtered log X-ray image, showing the gradient on scales of 16 arcsec.

5. Sloshing and instabilities

Fig. 4 (left and centre panels) show the fractional difference from the radial average of adaptively smoothed Chandra images of the cluster. In the centre we see a spiral structure. This is cooler and denser gas within the intracluster medium. In addition, there is a strong enhancement on surface brightness 8 arcmin to the east of the cluster core, and 4 arcmin to the west of the cluster core. On larger scales there is a east-west asymmetry in the X-ray surface brightness (Churazov *et al.* 2003).

Spiral structures and alternating enhancements and decrements in surface brightness and temperature are characteristic of gas sloshing within the potential well of a cluster (for a review see Markevitch & Vikhlinin 2007). These regions are separated by contact discontinuities where the pressure is continuous, but the temperature and temperature jump.

Several such features are seen in Perseus. These edges in surface brightness and temperature are seen out to 700 kpc radius (Simionescu *et al.* 2012; Urban *et al.* 2014). There is a chain of galaxies in the western side of the cluster which may be responsible for the generation of the sloshing (Churazov *et al.* 2003).

The concave-shaped Bay region to the south could be an ancient cavity (e.g. Fabian *et al.* 2011), although there is no associated low frequency radio emission. Another possibility might be that it is a 50 kpc roll generated by Kelvin-Helmholtz instabilities

https://doi.org/10.1017/S1743921318005756 Published online by Cambridge University Press

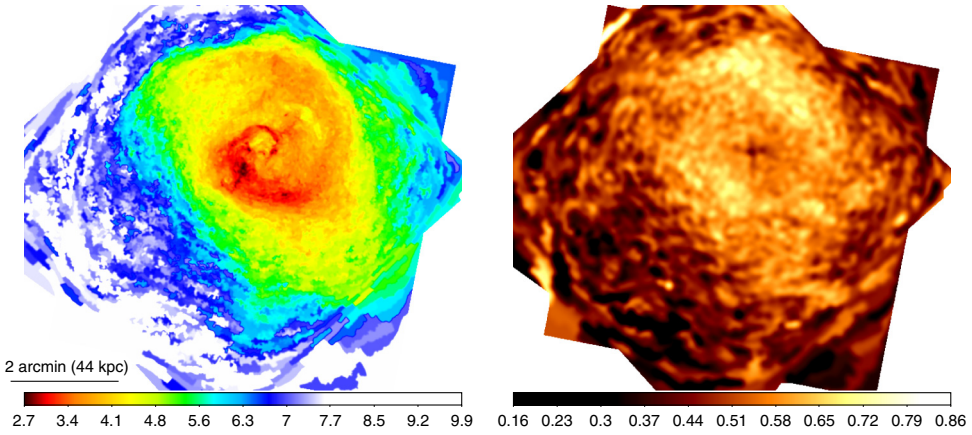

Figure 5. Temperature and metallicity maps, created by spectral fitting spectra from regions containing 10^4 counts (Sanders & Fabian 2007). The maps have been smoothed by Gaussians of 2 and 8 arcsec, respectively. The units of temperature are keV and the metallicity $Z_\odot$.

(Walker *et al.* 2017). If so, comparisons with simulations suggest that a magnetic field pressure of $\beta = 200$ is required to reproduce this feature.

6. Larger scale structures

Also on large scales to the north (Fig. 4) are several depressions in surface brightness (Sanders & Fabian 2007). The largest of these to the north (known as the northern trough; Fabian *et al.* 2011) is a 10 per cent drop in surface brightness and lies along the main jet axis to the north and is also along the axis of the long Hα filament. It is plausible that the trough may be the cavity associated with bubbles which dragged out this filament. If so, then it would be equivalent in energy (estimated using $4PV$ enthalpy) of 11 of the bubbles in the centre ($\sim 10^{60}$ erg). Alternatively, it might be the accumulation of several episodes of feedback. The radio mini halo of the cluster also extends in this northern direction to the radius of the northern trough (Fabian *et al.* 2011).

The entire core of the cluster is surrounded by an egg-shaped region of several hundred kpc radius (Fig. 4 right panel). There is, in particular, a very sharp gradient to the south-west of the nucleus. The edge of the radio mini halo also located here. It is unclear what the origin of this structure is, as a cold front would not be expected to be on all sides of the cluster.

7. The metallicity distribution

The centre of the cluster shows a strong metal enhancement, though the metallicity declines in the innermost 20 kpc (Fig. 5). This does not appear to be a bias due to inadequate modelling of the spectrum (Sanders & Fabian 2007). There are also blobs of high metallicty gas (e.g. 40 kpc to the south-west of the cluster core). These have scales of ~ 5 kpc and total $\sim 3 \times 10^4$ $M_\odot$ of excess iron.

One explanation is that these are high metallicity material which is dragged out by a rising cavity in the cluster. The spatial connection between the cavities and metals in Perseus, is however, not that clear. In a sample of systems a connection is found between the radius of the metals and jet power (Kirkpatrick & McNamara 2015).

The presence of these blobs shows they must be able to survive within the ICM for reasonable timescales, also providing additional constrains on the motions of the gas (e.g. Rebusco *et al.* 2005; Graham *et al.* 2006).

https://doi.org/10.1017/S1743921318005756 Published online by Cambridge University Press

References

Böhringer, H., Voges, W., Fabian, A. C., Edge, A. C., & Neumann, D. M. 1993, *MNRAS*, 264, L25
Branduardi-Raymont, G., Fabricant, D., Feigelson, E., *et al.* 1981, *ApJ*, 248, 55
Churazov, E., Forman, W., Jones, C., & Böhringer, H. 2003, *ApJ*, 590, 225
Churazov, E., Sunyaev, R., Forman, W., & Böhringer, H. 2002, *MNRAS*, 332, 729
Conselice, C. J., Gallagher, III, J. S., & Wyse, R. F. G. 2001, *AJ*, 122, 2281
Croston, J. H., Sanders, J. S., Heinz, S., *et al.* 2013, ArXiv e-prints, arXiv:1306.2323
Fabian, A. C. 2012, *ARA&A*, 50, 455
Fabian, A. C., Celotti, A., Blundell, K. M., Kassim, N. E., & Perley, R. A. 2002, *MNRAS*, 331, 369
Fabian, A. C., Hu, E. M., Cowie, L. L., & Grindlay, J. 1981, *ApJ*, 248, 47
Fabian, A. C., Sanders, J. S., Allen, S. W., *et al.* 2011, *MNRAS*, 418, 2154
Fabian, A. C., Sanders, J. S., Allen, S. W., *et al.* 2003a, *MNRAS*, 344, L43
Fabian, A. C., Sanders, J. S., Crawford, C. S., *et al.* 2003b, *MNRAS*, 344, L48
Fabian, A. C., Sanders, J. S., Ettori, S., *et al.* 2000, *MNRAS*, 318, L65
Fabian, A. C., Sanders, J. S., Taylor, G. B., *et al.* 2006, *MNRAS*, 366, 417
Fabian, A. C., Walker, S. A., Russell, H. R., *et al.* 2017, *MNRAS*, 464, L1
Ferland, G. J., Fabian, A. C., Hatch, N. A., *et al.* 2009, *MNRAS*, 392, 1475
Gendron-Marsolais, M., Hlavacek-Larrondo, J., Martin, T. B., *et al.* 2018, *MNRAS*, 479, L28
Gillmon, K., Sanders, J. S., & Fabian, A. C. 2004, *MNRAS*, 348, 159
Graham, J., Fabian, A. C., Sanders, J. S., & Morris, R. G. 2006, *MNRAS*, 368, 1369
Graham, J., Sanders, J. S., & Fabian, A. C. 2008, *MNRAS*, 386, 278
Hatch, N. A., Crawford, C. S., Johnstone, R. M., & Fabian, A. C. 2006, *MNRAS*, 367, 433
Kent, S. M. & Sargent, W. L. W. 1979, *ApJ*, 230, 667
Kirkpatrick, C. C. & McNamara, B. R. 2015, *MNRAS*, 452, 4361
Markevitch, M. & Vikhlinin, A. 2007, *Phys. Rep.*, 443, 1
Rebusco, P., Churazov, E., Böhringer, H., & Forman, W. 2005, *MNRAS*, 359, 1041
Ruszkowski, M., Brüggen, M., & Begelman, M. C. 2004, *ApJ*, 611, 158
Sanders, J. S. & Fabian, A. C. 2007, *MNRAS*, 381, 1381
Sanders, J. S., Fabian, A. C., Russell, H. R., Walker, S. A., & Blundell, K. M. 2016, *MNRAS*, 460, 1898
Sijacki, D. & Springel, V. 2006, *MNRAS*, 366, 397
Simionescu, A., Werner, N., Urban, O., *et al.* 2012, *ApJ*, 757, 182
Urban, O., Simionescu, A., Werner, N., *et al.* 2014, *MNRAS*, 437, 3939
Walker, S. A., Hlavacek-Larrondo, J., Gendron-Marsolais, M., *et al.* 2017, *MNRAS*, 468, 2506
Weisskopf, M. C., Brinkman, B., Canizares, C., *et al.* 2002, *PASP*, 114, 1
Zhuravleva, I., Churazov, E., Schekochihin, A. A., *et al.* 2014, *Nature*, 515, 85